# Prediction of Diffuser Core Flow Fluctuations Caused by Oscillating Turbulent Flow

A. Schachenmann* and D.O. Rockwell†
*Lehigh University, Bethlehem, Pa.*

**Theoretical consideration of the time-dependent diffuser core flow, involving two limiting models (high-frequency and low-frequency) for the time-dependent effective core flow area, results in predictions for decay of the first harmonic core velocity and wall pressure amplitudes with streamwise distance. In order to predict these decays, it is necessary to specify only time mean core flow and either time-dependent diffuser inlet or exit conditions. The theoretical models are compared with experiments for diffuser inlet conditions, spanning a ten-fold range of dimensionless frequencies. The high-frequency model best predicts the decay of core velocity fluctuations and wall pressure fluctuations in the streamwise direction. A backward calculation scheme, which uses diffuser exit conditions as initial conditions, enables good prediction of the fluctuating wall pressure distributions when the diffuser exit exhausts into the atmosphere. An order-of-magnitude analysis yields a simple expression for decay of the core velocity fluctuations when the dimensionless frequency is approximately unity.**

## Nomenclature

$a$ = piston radius
$A$ = geometric area
$A_f$ = flow area
$\bar{A}_f$ = time mean flow area
$\tilde{A}_f$ = flow area fluctuation
$A^*$ = blocked area
$\bar{A}^*$ = time mean blocked area
$\tilde{A}^*$ = blocked area fluctuation
$B$ = complex amplitude of flow area fluctuation
$c$ = speed of sound
$D$ = diffuser diameter
$\bar{E}$ = blockage factor = $\bar{A}_f/A$
$i$ = $\sqrt{-1}$
$k$ = $\omega/c$
$M_s$ = effective mass
$p$ = static pressure
$\bar{p}$ = mean static pressure
$\tilde{p}$ = static pressure fluctuation
$P$ = complex amplitude of static pressure fluctuation
$r$ = radial coordinate
$R$ = diffuser radius
$Re$ = Reynolds number = $(\bar{u}_0 D)/\nu$
$St_L$ = frequency parameter, Strouhal number = $(\omega L)/\bar{u}_0$
$t$ = time
$u$ = velocity
$\bar{u}$ = mean velocity
$\tilde{u}$ = velocity fluctuation
$u_\ell$ = centerline velocity
$U$ = complex amplitude of velocity fluctuation
$x$ = axial coordinate
$y$ = distance from wall
$\rho$ = density
$\bar{\rho}$ = mean density
$\tilde{\rho}$ = density fluctuation
$\omega$ = radian frequency of oscillation
$\delta^*$ = boundary-layer displacement thickness
$\theta$ = boundary-layer momentum thickness
$\Delta$ = variation
$\phi$ = phase angle

*Subscripts*

$0$ = diffuser inlet
$1$ = diffuser exit

Received Sept. 1, 1977; revision received Jan. 12, 1978. Presented as Paper 76-GT-76 at the 1976 ASME Gas Turbine Conference. 

Index categories: Nonsteady Aerodynamics; Nozzle and Channel Flow.

*Visiting Assistant Professor, Department of Mechanical Engineering and Mechanics.

†Professor, Department of Mechanical Engineering and Mechanics. Associate Member AIAA.

## Introduction

The propagation of organized oscillations through diffusers occurs in a number of turbomachinery systems. For example, stator flow passages are subjected to oscillatory flow generated by the passing rotor blade wakes; the diffuser downstream of the compressor in a gas turbine experiences oscillatory flow; the vaned diffuser section of a centrifugal compressor undergoes periodic flow due to the impeller blade wakes. An understanding of the oscillating turbulent flow in an unstalled diffuser requires study of the time-dependent inviscid core flow. Outside the boundary layer of such a diffuser flow, the core flow pressure, velocity, and effective flow variation with time at a given axial position impose conditions on the boundary layer which dictate its time-dependent growth. Since the diffuser flowfield is an internal one, the variation of the core flow parameters is coupled with behavior of the boundary layer. Thus, an exact independent specification of the core flow is not possible. This investigation focuses on development of an approximate core flow model, enabling independent prediction of the time-dependent core flow when the time mean core flow and time-dependent diffuser inlet conditions are prescribed. The time mean core flow can be predicted using one of the currently available step-by-step numerical boundary-layer prediction methods.

The most closely related previous investigations consider two basic classes of unsteady internal flow problems: unsteady fully developed turbulent flow and unsteady inviscid flow. Regarding the former class of flows, Brown et al.[1] examined in detail fully developed turbulent flow in long constant-area lines, and Strunk[2] carried out the analogous study for laminar flow. Earlier references are cited in both of these works. Concerning the latter class of flows, Whitehead,[3] Powell,[4] Eisenberg and Kao,[5] and Chiang et

al.[6] studied the inviscid small-amplitude disturbance propagation through various sorts of ducts. No attention has been given to the situation of oscillating internal flow, where at any cross section of the flow there exists an inviscid core surrounded by a boundary layer of substantial thickness. The present study involves use of the experimental techniques described in Ref. 7 and formulation of a theoretical core model to give insight into such core flow behavior.

## Core Flow Theory

As shown in Fig. 1, the problem is posed as a quasi-one-dimensional, isentropic core of cross-sectional area $A_f$ nested within a time-dependent boundary-layer displacement area indicated by the cross-hatched region. The cross-sectional area of the flow occupied by the integrated boundary-layer displacement area is given by $A-A_f$. Figure 2 defines the notation for the core velocity and wall pressure fluctuation amplitudes, along with corresponding phase angles.

At a given location in the diffuser core, the continuity and momentum equations read

$$\frac{\partial(\rho A)}{\partial t}+\frac{\partial(\rho u A_f)}{\partial x}=0 \tag{1}$$

$$\frac{\partial u}{\partial t}+u\frac{\partial u}{\partial x}=-\frac{1}{\rho}\frac{\partial p}{\partial x} \tag{2}$$

Writing the corresponding steady-state equations,

$$\frac{\mathrm{d}}{\mathrm{d}x}(\bar{\rho}\bar{u}\bar{A}_f)=0 \tag{3}$$

$$\bar{u}\frac{\mathrm{d}\bar{u}}{\mathrm{d}x}=-\frac{1}{\bar{\rho}}\frac{\mathrm{d}\bar{p}}{\mathrm{d}x} \tag{4}$$

Relation mean flow area to mean velocity in the diffuser core by use of the continuity equation (3),

$$\bar{\rho}\bar{u}\frac{\mathrm{d}\bar{A}_f}{\mathrm{d}x}+\bar{\rho}\bar{A}_f\frac{\mathrm{d}\bar{u}}{\mathrm{d}x}+\bar{u}\bar{A}_f\frac{\mathrm{d}\bar{\rho}}{\mathrm{d}x}=0 \tag{5}$$

using the isentropic equation for speed of sound,

$$\frac{\mathrm{d}\bar{p}}{\mathrm{d}\bar{\rho}}=c^2 \tag{6}$$

and

$$\frac{\mathrm{d}\bar{\rho}}{\mathrm{d}x}=\frac{\mathrm{d}\bar{p}}{\mathrm{d}x}\frac{1}{c^2}=-\bar{\rho}\bar{u}\frac{\mathrm{d}\bar{u}}{\mathrm{d}x}\frac{1}{c^2}$$

and solving for $(1/\bar{A}_f)\ (\mathrm{d}\bar{A}_f/\mathrm{d}x)$, it follows that

$$\frac{1}{\bar{A}_f}\frac{\mathrm{d}\bar{A}_f}{\mathrm{d}x}=-\frac{1}{\bar{u}}\frac{\mathrm{d}\bar{u}}{\mathrm{d}x}\left(1-\frac{\bar{u}^2}{c^2}\right) \tag{7}$$

As an approximation, the flow parameters can now be considered sums of a steady component and an unsteady component:

$$u(x,t)=\bar{u}(x)+\tilde{u}(x,t) \qquad (\bar{u}\gg\tilde{u}) \tag{8a}$$

$$p(x,t)=\bar{p}(x)+\tilde{p}(x,t) \qquad (\bar{p}\gg\tilde{p}) \tag{8b}$$

$$A_f(x,t)=\bar{A}_f(x)+\tilde{A}_f(x,t) \qquad (\bar{A}_f\gg\tilde{A}_f) \tag{8c}$$

$$\rho(x,t)=\bar{\rho}(x)+\tilde{\rho}(x,t) \qquad (\bar{\rho}\gg\tilde{\rho}) \tag{8d}$$

Writing the continuity and momentum equations, neglecting terms of second order, and using the steady-state equations (3 and 4), new forms of the continuity and momentum equations result:

$$A\frac{\partial\tilde{\rho}}{\partial t}+\frac{\partial}{\partial x}(\bar{\rho}\tilde{u}\bar{A}_f+\bar{\rho}\bar{u}\tilde{A}_f+\tilde{\rho}\bar{u}\bar{A}_f)=0 \tag{9}$$

$$\frac{\partial\tilde{u}}{\partial t}+\bar{u}\frac{\partial\tilde{u}}{\partial x}+\tilde{u}\frac{\partial\bar{u}}{\partial x}=-\frac{1}{\bar{\rho}}\frac{\partial\tilde{p}}{\partial x}+\frac{\tilde{\rho}}{\bar{\rho}^2}\frac{\partial\bar{p}}{\partial x} \tag{10}$$

For small values of $\tilde{\rho}$ and $\tilde{p}$, the following approximation can be made:

$$\frac{\mathrm{d}p}{\mathrm{d}\rho}\approx\frac{\tilde{p}}{\tilde{\rho}}\approx c^2 \tag{11}$$

Carrying out the differentiation of Eq. (9) and using Eq. (11),

$$\frac{A}{c^2}\frac{\partial\tilde{p}}{\partial t}+\frac{\bar{A}_f\bar{u}}{c^2}\frac{\mathrm{d}\tilde{p}}{\mathrm{d}x}+\bar{A}_f\bar{\rho}\frac{\mathrm{d}\tilde{u}}{\mathrm{d}x}+\bar{\rho}\bar{u}\frac{\partial\tilde{A}_f}{\partial x}+\frac{\tilde{A}_f\bar{u}}{c^2}\frac{\mathrm{d}\bar{p}}{\mathrm{d}x}+\tilde{A}_f\bar{\rho}\frac{\partial\bar{u}}{\partial x}+\bar{\rho}\bar{u}\frac{\mathrm{d}\tilde{A}_f}{\mathrm{d}x}+\frac{\tilde{A}_f\bar{u}}{c^2}\frac{\partial\bar{p}}{\partial x}+\frac{\tilde{A}_f\tilde{p}}{c^2}\frac{\mathrm{d}\bar{u}}{\mathrm{d}x}+\frac{\tilde{p}\bar{u}}{c^2}\frac{\mathrm{d}\bar{A}_f}{\mathrm{d}x}=0 \tag{12}$$

Dividing Eq. (12) by $A$, using Eqs. (4, 7, and 11), and defining

$$\tilde{E}\equiv\tilde{A}_f/A \tag{13}$$

Eq. (12) becomes

$$\frac{1}{c^2}\frac{\partial\tilde{p}}{\partial t}+\frac{\bar{\rho}\bar{u}}{A}\frac{\partial\tilde{A}_f}{\partial x}+\frac{\tilde{E}\bar{u}}{c^2}\frac{\partial\bar{p}}{\partial x}+\tilde{E}\bar{\rho}\frac{\partial\bar{u}}{\partial x}+\left[\frac{\tilde{A}_f}{A}\bar{\rho}\left(1-\frac{\bar{u}^2}{c^2}\right)+\frac{\tilde{p}\bar{u}^2\tilde{E}}{c^4}-\frac{\tilde{p}\bar{u}\tilde{E}}{\bar{u}}\right]\frac{\mathrm{d}\bar{u}}{\mathrm{d}x}=0 \tag{14}$$

Similarly, the momentum Eq. (10) becomes

$$\frac{\partial\tilde{u}}{\partial t}+\bar{u}\frac{\partial\tilde{u}}{\partial x}+\frac{1}{\bar{\rho}}\frac{\partial\tilde{p}}{\partial x}+\left[\tilde{u}+\frac{\tilde{p}\bar{u}}{c^2\bar{\rho}}\right]\frac{\mathrm{d}\bar{u}}{\mathrm{d}x}=0 \tag{15}$$

Now assuming that the perturbations are harmonic,

$$\tilde{u}=Ue^{i\omega t} \qquad \tilde{p}=Pe^{i\omega t} \qquad \tilde{A}_f=Be^{i\omega t} \tag{16}$$

where $U$, $P$, $B$ are complex.

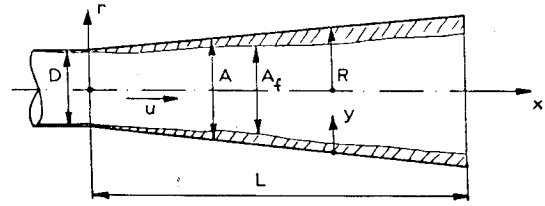


**Fig. 1 Schematic of diffuser core flow.**

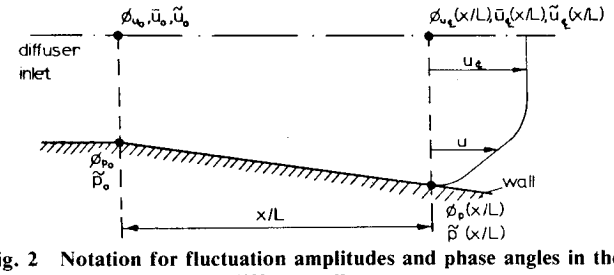


**Fig. 2 Notation for fluctuation amplitudes and phase angles in the diffuser core and along the diffuser wall.**

Inserting Eq. (16) into the momentum Eq. (15) and the continuity Eq. (14),

$$\frac{i\omega}{c^2}P+\frac{\bar{\rho}\bar{u}dB}{Adx}+\frac{\bar{E}\bar{u}dP}{c^2dx}+\bar{E}\bar{\rho}\frac{dU}{dx}$$
$$+\left[\frac{B}{A}\bar{\rho}\left(1-\frac{\bar{u}^2}{c^2}\right)+\frac{P\bar{u}^2\bar{E}}{c^4}-\frac{\bar{\rho}\bar{E}U}{\bar{u}}\right]\frac{d\bar{u}}{dx}=0 \quad (17)$$

and

$$i\omega U+\bar{u}\frac{dU}{dx}+\left[U+\frac{P\bar{u}}{c^2\bar{\rho}}\right]\frac{d\bar{u}}{dx}+\frac{1}{\bar{\rho}}\frac{dP}{dx}=0 \quad (18)$$

Solving Eq. (18) for $dP/dx$, substituting the resultant expression into Eq. (17), then solving for $dU/dx$, we have

$$\frac{dU}{dx}=\left\{\frac{1}{\bar{E}(1-\bar{u}^2/c^2)}\right\}\left\{U\left[\bar{E}\left(1+\frac{\bar{u}^2}{c^2}\right)\frac{1}{\bar{u}}\frac{d\bar{u}}{dx}+\frac{\bar{u}\bar{E}}{c^2}i\omega\right]\right.$$
$$\left.-\frac{\bar{u}}{A}\frac{dB}{dx}-\frac{B}{A}\left(1-\frac{\bar{u}^2}{c^2}\right)\frac{d\bar{u}}{dx}-\frac{i\omega P}{\bar{\rho}c^2}\right\} \quad (19)$$

Now, solving Eq. (18) for $dU/dx$, substituting the expression into Eq. (17), and solving the resultant equation for $(1/\bar{\rho})(dP/dx)$, we have

$$\frac{1}{\bar{\rho}}\frac{dP}{dx}=\left\{\frac{1}{\bar{E}(1-\bar{u}^2/c^2)}\right\}\left\{-U\bar{E}\left(i\omega+2\frac{d\bar{u}}{dx}\right)\right.$$
$$+\frac{P\bar{u}}{\bar{\rho}c^2}\left[i\omega-\bar{E}\left(1-\frac{\bar{u}^2}{c^2}\right)\frac{d\bar{u}}{dx}\right]$$
$$\left.+\frac{\bar{u}^2dB}{Adx}+\frac{B}{A}\bar{u}\left(1-\frac{\bar{u}^2}{c^2}\right)\frac{d\bar{u}}{dx}\right\} \quad (20)$$

Equations (19) and (20) are two coupled differential equations for the velocity, pressure, and area perturbation amplitudes $U$, $P$, $B$. In order to solve these equations, it is necessary to specify the time mean core flow and the flow area perturbation $B$. Since it is desirable to be able to predict the time-dependent core flow a priori for a specified mean flow, two simple models for the flow area perturbation $B$ will be considered. In essence, formulation of these models requires physical approximation for the behavior of the time-dependent boundary-layer.

The extensive theoretical and experimental information available for unsteady laminar boundary layers can provide a cue for the high-frequency behavior of the unsteady turbulent boundary layer. According to Lin,[8] the "ac" boundary-layer behavior is decoupled from the time mean boundary layer if $(\delta_{ac}/\delta)^2 \ll 1$, where $\delta_{ac}=\sqrt{2\nu/\omega}$. For the highest frequency (35 Hz) considered herein, $(\delta_{ac}/\delta)^2=2.5\times10^{-3}\ll1$. It should be noted that the effective value of viscosity for turbulent flow is greater than $\nu$, so this criterion is only an approximation. This tendency for decoupling leads to the high-frequency assumption proposed here. The core flow oscillations are assumed to penetrate the time mean turbulent boundary layer to the wall unaltered, and the influence of any turbulent "ac" layer is neglected. Equations (A10) and (A11) of the Appendix give the required manipulations to arrive at the expressions for the high-frequency flow area perturbation and its streamwise gradient

At very low frequencies and small amplitudes of oscillation, the behavior of the boundary layer should be quasisteady. The local velocity fluctuation amplitude in the boundary layer is assumed proportional to the local time mean velocity in the boundary layer. If the instantaneous boundary-layer displacement thickness made dimensionless with respect to diffuser radius $R$ is defined, the displacement thickness is invariant for all time, as long as the proportionality between local fluctuation and time mean velocity holds. Since displacement thickness is invariant, $B=0$ and $dB/dx=0$. This sort of low-frequency behavior is approximated, for example, by the low-frequency disturbance boundary-layer profiles of Ref. 7.

Substitution of the expressions for the high- and low-frequency flow area perturbation models in Eq. (19) and (20) yields, after manipulation, the following sets of simultaneous equations for the velocity and pressure perturbation amplitudes. For the high-frequency approximation,

$$\frac{dU}{dx}=\left\{\frac{1}{1-\bar{E}\bar{u}^2/c^2}\right\}\left[U\left\{\frac{1}{\bar{u}}\frac{d\bar{u}}{dx}\left(\bar{E}+\frac{\bar{u}^2}{c^2}\right)+\frac{\bar{E}\bar{u}i\omega}{c^2}\right.\right.$$
$$\left.\left.-(1-\bar{E})\frac{1}{A}\frac{dA}{dx}+\frac{d\bar{E}}{dx}\right\}-\frac{i\omega P}{\bar{\rho}c^2}\right] \quad (21)$$

$$\frac{1}{\bar{\rho}}\frac{dP}{dx}=\left\{\frac{1}{\bar{E}(1-\bar{u}^2/c^2)}\right\}\left[-\bar{E}U\left(i\omega+2\frac{d\bar{u}}{dx}\right)\right.$$
$$+\frac{P\bar{u}}{\bar{\rho}c^2}\left\{i\omega-\bar{E}\left(1-\frac{\bar{u}^2}{c^2}\right)\frac{d\bar{u}}{dx}\right\}$$
$$+U(1-\bar{E})\left(1-\frac{\bar{u}^2}{c^2}\right)\frac{d\bar{u}}{dx}+\bar{u}\left\{\frac{dU}{dx}(1-\bar{E})\right.$$
$$\left.\left.+U(1-\bar{E})\left(\frac{1}{A}\frac{dA}{dx}-\frac{1}{\bar{u}}\frac{d\bar{u}}{dx}\right)-U\frac{d\bar{E}}{dx}\right\}\right] \quad (22)$$

For the low-frequency approximation,

$$\frac{dU}{dx}=\left\{\frac{1}{\bar{E}(1-\bar{u}^2/c^2)}\right\}$$
$$\times\left[\bar{E}U\left\{\left(1+\frac{\bar{u}^2}{c^2}\right)\frac{1}{\bar{u}}\frac{d\bar{u}}{dx}+\frac{\bar{u}}{c^2}i\omega\right\}-\frac{i\omega P}{\bar{\rho}c^2}\right] \quad (23)$$

$$\frac{1}{\bar{\rho}}\frac{dP}{dx}=\left\{\frac{1}{\bar{E}(1-\bar{u}^2/c^2)}\right\}$$
$$\times\left[-\bar{E}U\left(i\omega+2\frac{d\bar{u}}{dx}\right)+\frac{P\bar{u}}{\bar{\rho}c^2}\left\{i\omega-\bar{E}\left(1-\frac{\bar{u}^2}{c^2}\right)\frac{d\bar{u}}{dx}\right\}\right] \quad (24)$$

Either set of simultaneous differential equations can be solved numerically to yield the pressure and velocity perturbation amplitudes by specifying only the time mean core flow velocity and area, the geometric area of the diffuser, and the frequency of the applied oscillation. Detailed discussion of the solution procedure appears in Ref. 7. A numerical marching type of solution was used. This involved starting at the diffuser inlet and marching downstream or at the diffuser exit and marching upstream. The former is termed a forward calculation scheme and the latter a backward calculation scheme.

An order-of-magnitude analysis of each of the terms in the simultaneous Eqs. (21) and (22) reveals a particularly simple expression for the velocity perturbation amplitude, where the limiting value of dimensionless frequency $St_L \simeq 1$ and the order of magnitude of each of the physical variables is $U\sim U$, $P\sim P$, $\bar{E}=A_f/A\sim1$, $A\sim L^2$, $x\sim L$, $\bar{\rho}\sim\rho u_0^2$, $\bar{u}\sim u_0$, and $\bar{u}^2/c^2\sim u_0^2/c^2\ll1$, where $u_0$ is the time mean value of the diffuser inlet velocity. Using the definition of dimensionless frequency, $St_L=\omega L/u_0$, assuming that $(u_0/c)^2\ll1$, and retaining terms of order $U/L$ and the pressure term, Eq. (21) becomes

$$\frac{d}{dx}U\approx U\frac{1}{\bar{u}}\frac{d\bar{u}}{dx}\left(\bar{E}+\frac{\bar{u}^2}{c^2}\right)+U\frac{d\bar{E}}{dx}-\frac{i\omega P}{\bar{\rho}c^2} \quad (25)$$

The order of the pressure term remains for evaluation. Considering Eq. (22), an order-of-magnitude analysis followed by considerable manipulation yields an approximation for the magnitude of the pressure amplitude in terms of velocities $P/\rho \sim u_0 U$. So the pressure term in Eq. (25) takes the form

$$\frac{i\omega P}{\rho c^2} \sim St_L \frac{u_0}{L} \frac{l}{c^2} \frac{P}{\rho} \sim \left(St_L \frac{u_0^2}{c^2}\right) \frac{U}{L}$$

It is evident that this pressure term is much smaller than the other terms in Eq. (21), so the approximate differential equation for the velocity perturbation amplitude becomes

$$\frac{dU}{dx} \simeq U \frac{l}{\bar{u}} \frac{d\bar{u}}{dx} + U \frac{d\bar{E}}{dx}$$

Integrating and using the known time mean conditions at the diffuser inlet ($\bar{u}_0$ and $\bar{E}$ at $x=0$), the decay of the velocity perturbation follows:

$$U \simeq (\bar{u}/\bar{u}_0) U_0 \exp(\bar{E} - \bar{E}_0)$$

This decay, which is independent of frequency of oscillation, is limited to the case where the dimensionless frequency approaches unity, the diffuser inlet velocity is an order less than the speed of sound, and the diffuser flow area is the same order as the geometrical area.

## Experimental Results

Use of the experimental techniques described in Ref. 7 enabled measurement of the first harmonic of the organized wall pressure and core flow velocity fluctuation amplitude and phase. The technique for measuring these organized components in the turbulent flow is similar to that used by Hussain and Reynolds[9] for a perturbed fully developed turbulent channel flow. In short, the measured wall pressure fluctuations and core flow velocity fluctuations were subjected to a phase-averaging process in order to extract the amplitude and phase of the organized pressure and velocity fluctuations. This extraction process was necessary, since the applied organized (essentially sinusoidal) disturbance at the diffuser inlet was super-imposed on background random turbulence as it propagated downstream through the diffuser. These extracted pressure and velocity amplitudes are denoted by $\tilde{p}$ and $\tilde{u}$. Corresponding phase angles are denoted by $\phi_p$ and $\phi_u$. For these experiments, the range of dimensionless frequency $0.63 \sim St_L \leq 7.33$ $[0.86 \times 10^{-3} \leq (St_{\theta_0})_{\text{inlet}} \leq 5.28 \times 10^{-3} (0 \leq f \leq 35$ Hz)] and $\tilde{u}_0/\bar{u}_0 \leq 0.10$ were examined. Average time mean inlet Reynolds number was $Re = 1.55 \times 10^5$ (Mach number $= 0.044$), and time mean displacement and momentum thicknesses were $\delta_0^*/R = 0.012$ and $\theta_0/R = 0.101$, respectively. The diffuser, which was smoothly faired at its inlet, had an included angle of 12 deg and an inlet diameter of 6 in. Measurements indicated that no flow separation was present.

Since evaluation of Eqs. (21-24) requires knowledge of the time mean core flow, it is essential to specify the degree of alteration of time mean core flow and boundary-layer parameters, relative to a zero applied oscillation state, when an oscillation of defined frequency and amplitude is generated at the diffuser inlet. Detailed measurements of the mean core flow and boundary layers,[7] subjected to the aforementioned spectrum of frequencies and amplitudes of interest in this study, revealed insignificant alteration of the undisturbed time mean flowfield. In addition, the root mean square of the core flow velocity fluctuations, in the absence of the applied oscillation, was measured to be of the order of 2% of the time mean core velocity.

The variations of core flow pressure amplitude, velocity amplitude, and phase with streamwise distance are referenced to the respective values at the diffuser inlet in the plots of Figs. 3-5. These three sets of plots are representative of the span of dimensionless frequencies ($St_L$) of interest on this study. Reference 7 gives additional intermediate data. For the variation of the core flow velocity fluctuation, both high- and low-frequency models are shown. There was insignificant difference between the forward and backward calculation schemes. However, for the variations of the wall pressure fluctuation, both forward and backward calculation schemes are shown. It was not possible to use the *measured* pressure at the diffuser exit as the initial condition for the backward calculation scheme because of its very low amplitude. This diffuser exit pressure fluctuation amplitude was determined from the accurately measured exit velocity fluctuation and an acoustic model using an effective diffuser exit air mass.[7] Of course, measured pressure and velocity fluctuation amplitudes at the diffuser inlet served as the initial conditions for the forward marching scheme. In summary, the backward calculation scheme accounts for the unsteady flow mismatch at the diffuser exit, whereas the forward calculation scheme does not.

At the lowest frequency (Fig. 3), the measured velocity fluctuation amplitudes fall within an envelope formed by the high- and low-frequency models. At the moderate and high frequencies (Figs. 4 and 5), the velocity amplitudes are

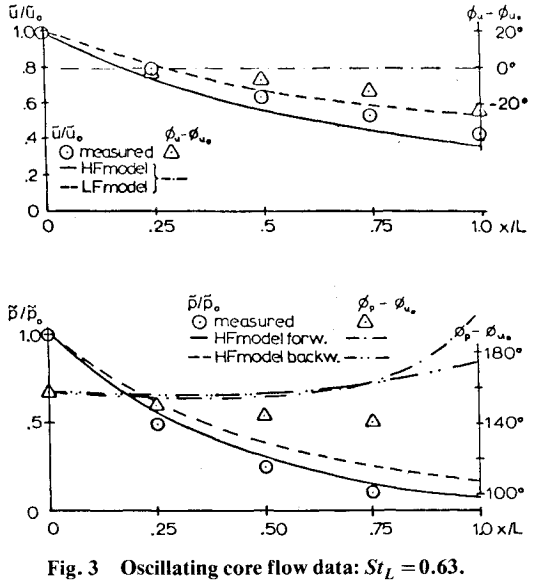


Fig. 3 Oscillating core flow data: $St_L = 0.63$.

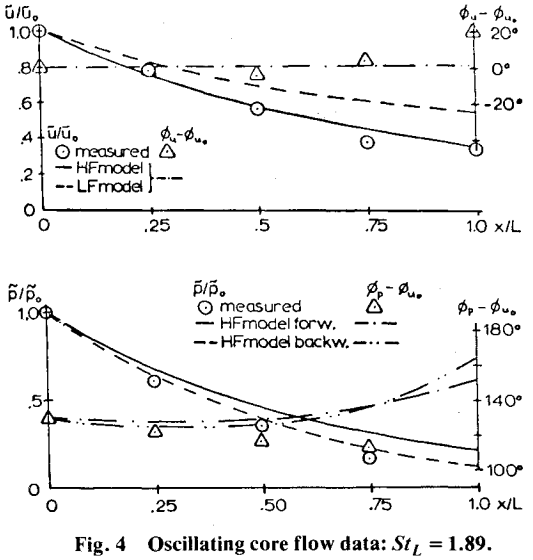


Fig. 4 Oscillating core flow data: $St_L = 1.89$.

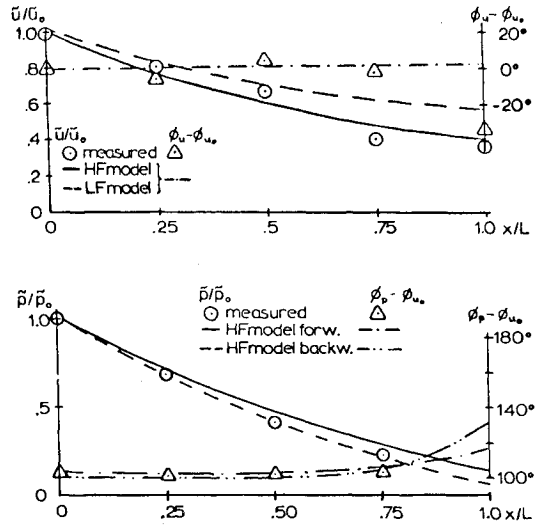


**Fig. 5 Oscillating core flow data: $St_L = 7.33$.**

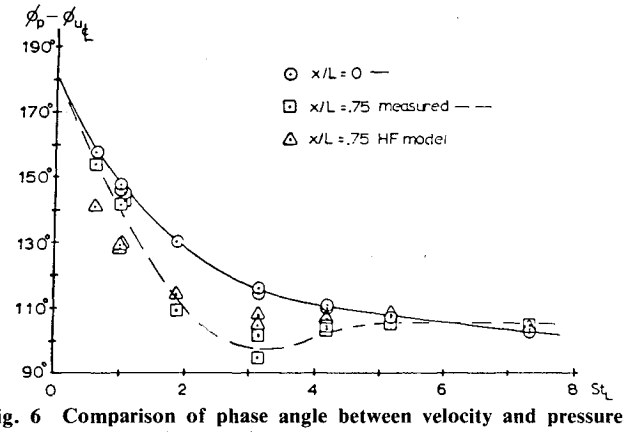


**Fig. 6 Comparison of phase angle between velocity and pressure fluctuations at different axial distances for a range of excitation frequencies.**

predicted well by the high-frequency model; pressure amplitudes are predicted best by the backward calculation scheme, which accounts for the mismatch at the diffuser exit, except at very low frequencies, where the acoustic model used to approximate the diffuser exit conditions becomes inaccurate.

Variation of amplitude and phase of the velocity oscillation within the boundary layer can cause deviations of the experimental pressure data from the high-frequency theroetical predictions (see boundary-layer data of Ref. 7). Writing the continuity equation for a control volume between the diffuser inlet and diffuser cross section of interest shows that amplifications of amplitude within the boundary layer, relative to local core flow, tend to produce experimental values below predicted values, and vice versa for amplitudes in the boundary layer smaller than local core values.

It is useful to compare the phase of the local pressure oscillation with that of the local velocity oscillation at a given value of $x/L$. The plot of Fig. 6 illustrates such a comparison at the locations $x/L = 0$ and $x/L = 0.75$. At high frequencies, the pressure oscillation leads the velocity oscillation by approximately 110 deg. This lead increases sharply at low values of dimensionless frequency ($St_L$).

## Conclusions

1) A high-frequency core flow model is capable of predicting the unsteady core flow characteristics when only the time mean core flow and the unsteady flow parameters at the diffuser inlet (or exit) are specified.

2) The predicted velocity amplitude decay is insensitive to diffuser exit conditions, whereas the predicted pressure amplitude decay at high dimensionless frequencies is sensitive and requires use of a backward calculation modification of the high-frequency model for accurate prediction.

3) Phase angle between wall pressure fluctuation and core velocity fluctuation at a given axial station is predicted well using the high-frequency model.

4) For the special case of dimensionless oscillation frequency approaching unity, a time mean core flow area the same order as the diffuser area, and a diffuser time inlet velocity an order smaller than the speed of sound, an order-of-magnitude analysis shows that the variation of the core flow fluctuation amplitude with streamwise distance reduces to a simple decay, which is independent of frequency of oscillation

## Appendix: High-Frequency Model for Time-Dependent Core Flow Area

For incompressible flow, the instantaneous core flow and blocked areas are

$$A_f = \int_0^R 2\pi r \frac{u}{u_\ell}\,dr \tag{A1}$$

$$A^* = A - A_f = \int_0^R 2\pi r\left[1 - \frac{u}{u_\ell}\right]dr \tag{A2}$$

Assuming small-amplitude harmonic oscillations, penetrating unchanged through the boundary layer,

$$A^* = \int_0^R 2\pi r\left[1 - \frac{\bar{u} + Ue^{i\omega t}}{\bar{u}_\ell + Ue^{i\omega t}}\right]dr$$

or

$$A^* = \frac{\bar{u}_\ell}{\bar{u}_\ell + Ue^{i\omega t}} \int_0^R 2\pi r\left[1 - \frac{\bar{u}}{\bar{u}_\ell}\right]dr$$

but

$$\bar{A}^* = \int_0^R 2\pi r\left[1 - \frac{\bar{u}}{\bar{u}_\ell}\right]dr \tag{A3}$$

so

$$A^* = \frac{\bar{A}^*}{1 + (U/\bar{u}_\ell)e^{i\omega t}} \tag{A4}$$

For small freestream oscillations, Eq. (A4) can be approximated as

$$A^* = \bar{A}^*[1 - (U/\bar{u}_\ell)e^{i\omega t}] \tag{A4a}$$

$$A^* = \bar{A}^* + \tilde{A}^* \tag{A5}$$

where the oscillating component of blocked area ($\tilde{A}^*$) is

$$\tilde{A}^* = -\bar{A}^*(U/\bar{u}_\ell)e^{i\omega t} \tag{A6}$$

From perturbing the equation $A^* = A - A_f$, it follows that

$$\tilde{A}_f = \bar{A}^*(U/\bar{u}_\ell)e^{i\omega t} \tag{A7}$$

Using Eq. (9), the mean blocked area can be expressed in terms of $E$:

$$\bar{A}^* = A - \bar{A}_f = A(1 - \bar{A}_f/A) = A(1 - \bar{E}) \tag{A8a}$$

$$\tilde{A}_f = A(1 - \bar{E})(U/\bar{u}_\ell)e^{i\omega t} \tag{A8b}$$

Using Eq. (10),

$$B=(1-\bar{E})A(U/\bar{u}_{\ell}) \tag{A9}$$

or, returning to the notation for the core flow in the main analysis,

$$B=(1-\bar{E})A(U/\bar{u}) \tag{A10}$$

and differentiating with respect to $x$,

$$\frac{dB}{dx}=\left(\frac{U}{\bar{u}}\right)\left[A\left(-\frac{d\bar{E}}{dx}\right)+\frac{dA}{dx}(1-\bar{E})\right]$$
$$+(1-\bar{E})A\left[\frac{1}{\bar{u}}\frac{dU}{dx}-\frac{U}{\bar{u}^2}\frac{d\bar{u}}{dx}\right] \tag{A11}$$

## Acknowledgments

The authors are grateful to the late Alan H. Stenning, who stimulated this effort, and to Forbes T. Brown, who suggested the diffuser exit model required for backward calculation. The authors thank J.J. Jaklitsch of the American Society of Mechanical Engineers for permission to publish this work.

## References

[1] Brown, F.T., Margolis, P.L., and Shah, R.D., "Small Amplitude Frequency Behavior of Fluid Lines with Turbulent Flow," *Journal of Basic Engineering,* Vol. 91, Dec. 1969, pp. 678-693.

[2] Strunk, R.D., "Frequency Response of Fluid Lines with Nonlinear Boundary Conditions," *Journal of Basic Engineering,* Vol. 93, Sept. 1971, pp. 365-372.

[3] Whitehead, D.S., "The Vibration of Air in a Duct with a Subsonic Mean Flow," *The Aeronautical Quarterly,* Vol. 12, Pt. 1, Feb. 1961, pp. 34-40.

[4] Powell, A., "Theory of Sound Propagation Through Ducts Carrying High-Speed Flows," *Journal of the Acoustical Society of America,* Vol. 32, Dec. 1960, pp. 1640-1646.

[5] Eisenberg, W.A. and Kao, T.W., "Propagation of Sound Through a Variable-Area Duct with a Steady Compressible Flow," *Journal of the Acoustical Society of America,* Vol. 49, Pt. 2, Jan. 1971, pp. 169-175.

[6] Chiang, T., Hsing, F.C., Pen, C.H.T., and Elrod, H.G., "Analysis of Pulsating Flows in Infinite and Finite Conical Nozzles," *Journal of Applied Mechanics,* Vol. 36, June 1969, pp. 159-170.

[7] Schachenmann, A.A., "Oscillating Turbulent Flow in a Conical Diffuser," Ph.D. Thesis, Dept. of Mechanical Engineering and Mechanics, Lehigh Univ., Bethlehem, Pa., 1974; also Schachenmann, A.A. and Rockwell, D.O., "Oscillating Turbulent Flow in a Conical Diffuser," *Journal of Fluids Engineering,* Vol. 98, Dec. 1976, pp. 695-701.

[8] Lin, C.C., "Motion in the Boundary Layer with Rapidly Oscillating External Flow," *Proceedings of the 9th International Congress of Applied Mechanics,* Vol. 4, 1957, Brussels, pp. 155-167.

[9] Hussain, A.K.M.F. and Reynolds, W.C., "The Mechanics of a Perturbation Wave in Turbulent Shear Flow," Thermosciences Div., Dept. of Mechanical Engineering, Stanford Univ., Rept. FM-6, May 1970; also *Journal of Fluid Mechanics,* Vol. 41, Pt. 2, April 1970, pp. 241-258; Vol. 54, Pt. 2, July 1972, pp. 241-288.